Transient Electro-Thermal Analysis of a Common Source Amplifier Circuit with a Physics-based MOSFET Model

Tao Pan, Dazhi Ding*, Hanxiang Li, and Xiaolin Cheng

Department of Communication Engineering, Nanjing University of Science and Technology, Nanjing, 210094, China
dzding@njust.edu.cn

Abstract **─** An algorithm that combines a common source amplifier with the physics-based metal-oxide-semiconductor field effect transistor (MOSFET) model is proposed. By solving the coupled drift-diffusion model equations with spectral element time-domain (SETD) method, the distribution of electron quasi-Fermi potential, hole quasi-Fermi potential and the potential inside the MOSFET is obtained. The corresponding current densities and electric intensities distributed in the device can be used to couple the heat conduction equation. Furthermore, the Kirchhoff laws should be satisfied when the MOSFET device is inserted in the circuit. The Newton-Raphson method is used to solve the nonlinear circuit equations due to the existence of semiconductor devices. The transient electro-thermal characteristics of a common source amplifier circuit have been analyzed, and the numerical results demonstrate the validity of the proposed method.

Index Terms **─** Amplifier, electro-thermal characteristics, MOSFET, SETD, transient simulation.

I. INTRODUCTION

The semiconductor devices are playing an increasingly important role in many practical applications. Under the actual work environment, the heat produced in the semiconductor not only increases energy consumption, will also have an impact on the performance of the device itself. Thereby, it is significant to execute the transient electro-thermal analysis of the semiconductor devices and circuits. To get an accurate description of the complex electrical characteristics of semiconductors, the equivalent-circuit-model-based and physical-model-based simulation are the two most common methods. However, the equivalent-circuit-models highly rely on the experiment measurements to persevere its validity for different semiconductor devices [1]-[3]. The physical-model-based multi-physics simulation is a preferred alternative method for the transient electro-thermal analysis of semiconductors, which equivalent-circuit-model expounded the transient physical process [4]-[6]. The drift-diffusion model (DDM) is a common way to describe the interior carrier behavior of semiconductors, and the heat conduction equation is intended for denoting the transient variation with temperature. The DDM can provide the distribution of heat source to the heat conduction equation, and the temperature change the mobility of carriers in return. [7] Research works [8-9] have been introduced to analyze the circuits including semiconductor devices, which are only for PIN diode with quasi one-dimension structure by finite difference method (FDM). The spectral element time-domain (SETD) method has shown its higher accuracy and lower computation cost than finite element method (FEM) or FDM [10-11], and received a rapid development in nanodevice simulation and computational electromagnetics [12-14].

In this paper, the transient electro-thermal characteristics of the semiconductors with the physics-based Model are analyzed by the SETD method. The electron and hole quasi-Fermi potential and electric potential are selected as the unknown variables for DDM, which is different from the traditional way [6-8]. The basic electro-thermal characteristics of a common source amplifier circuit with the MOSFET device has been analyzed which combined the physics-based multi-physics model and the circuit simulation.

In previous studies, we used electron concentration, hole concentration, and potential as variables. When studying complex models, if the mesh is not dense enough when simulating the breakdown characteristics, it will cause non-physical oscillations in electron concentration or hole concentration, and there will be a large number of negative values, resulting in solution divergence. However, if the mesh is too dense, the unknown will increase, the memory consumption and solution time will be increased, and the efficiency will be reduced.

The difference from the previous work is that the paper takes the electronic quasi-fee potential, the hole quasi-Fei potential and the potential as variables. The numerical distribution of the electron quasi-fee potential and the hole quasi-Fermi potential is small, and non-physical oscillation does not occur like the carrier

Submitted On: December 1, 2018
Accepted On: May 28, 2019

concentration. It is easier to converge without encrypting the mesh and ensuring the proper unknown.

The frame of this paper is as follows. In Section II, the physical model for semiconductors has been introduced briefly. The basic theory of SEM based on GLL (Gauss-Lobatto-Legendre) polynomials has been described for the physical model when the electron and hole quasi-Fermi potential and the potential are selected as the unknowns. The Newton iterative method is used to solve the nonlinear system of the circuits with semiconductors. In Section III, the transient electron-thermal characteristics of a common source amplifier circuit have been analyzed to demonstrate the validity with the proposed method. Finally the conclusion is given in Section IV.

II. PHYSICS-BASED MODEL AND NUMERICAL SCHEME

The drift-diffusion model equations [15, 16] are normalized as follows:

$$\mathbf{J}_n = -\mu_n n \nabla \phi_n , \tag{1}$$

$$\mathbf{J}_p = -\mu_p p \nabla \phi_p , \tag{2}$$

$$\frac{\partial n}{\partial t} = \nabla \cdot \mathbf{J}_n + G - R , \tag{3}$$

$$\frac{\partial p}{\partial t} = -\nabla \cdot \mathbf{J}_p + G - R , \tag{4}$$

$$\nabla^2 \varphi = (n - p - \Gamma), \tag{5}$$

where φ is the electrostatic potential, q is the electric charge, Γ is the electrically active net impurity concentration, and n and p are the electron and hole carrier densities. G and R describe the generation phenomena and recombination processes respectively. The relationships between the electron and hole quasi-Fermi potential and the electron and hole carrier densities are described as the following equations:

$$n = \exp[\varphi - \phi_n] , \tag{6}$$

$$p = \exp[\phi_p - \varphi] , \tag{7}$$

The heat conduction equation [16] is formulated as (8):

$$\frac{\partial T}{\partial t} = \frac{k_t}{\rho_m c_m} \nabla^2 T + \frac{P_d}{\rho_m c_m} , \tag{8}$$

$$P_d = -(\mathbf{J}_n + \mathbf{J}_p - \varepsilon \frac{\partial(\nabla\varphi)}{\partial t}) \cdot \nabla\varphi , \tag{9}$$

where ρ_m is the specific mass density, c_m is the specific heat capacity, k_t is the temperature dependent thermal conductivity, ε is the permittivity, and P_d is the inside heat generation rate described as formula (9).

A. SETD for semiconductor simulation

The difference between SEM and FEM lies in the choice of the expansion basis functions. In order to achieve the high accuracy, the GLL basis functions are employed throughout this article. The Nth order GLL basis functions in a 3-D cubic element $(\xi,\eta,\zeta) \in [-1,1]\times[-1,1]\times[-1,1]$ can be written as:

$$\Phi_{rst}(\xi,\eta,\zeta) = \phi_r^{(N_\xi)}(\xi)\phi_s^{(N_\eta)}(\eta)\phi_t^{(N_\zeta)}(\zeta) , \tag{10}$$

for $r = 0,1,\ldots,N_\xi; s = 0,1,\ldots,N_\eta; \mathrm{t} = 0,1,\ldots,N_\zeta$. $\phi_r^{(N_\xi)}(\xi)$, $\phi_s^{(N_\eta)}(\eta)$ and $\phi_t^{(N_\zeta)}(\zeta)$ represent the basis functions with three directions and have the following definition:

$$\phi_j^{(\mathrm{N})} = \frac{-1}{N(\mathrm{N}+1)\mathrm{L}_N(\xi_j)} \frac{(1-\xi^2)\mathrm{L}_N'(\xi)}{(\xi-\xi_j)} , \tag{11}$$

where $\mathrm{L}_N(\xi)$ and $\mathrm{L}_N'(\xi)$ are the Legendre polynomial of Nth order and its derivative. The points $\{\xi_j$, j=0,1,...,N$\}$ are the zeros of $(1-\xi^2)\mathrm{L}_N'(\xi_j)=0$. Because of the basis functions definition on the reference domain at the above standard cubic element, the mapping from the physical element to the reference domain is essential for general meshes [13-14].

Here, the electron and hole quasi-Fermi potential and electric potential are selected as the unknown variables. The fully coupled Newton iterative method is employed to solve the nonlinear equations. For the time partial derivative, the backward difference operator is employed to achieve the unconditional stability with a large time step size represented by Δt. The detail of the backward difference operated on the normalized electronic current continuity equation is given as the following:

$$F_n(\phi_n{}^m,\phi_p{}^m,\varphi^m) = f_n(\phi_n{}^m,\phi_p{}^m,\varphi^m)\cdot\Delta t - \left(\phi_n{}^m - \phi_p{}^{m-1}\right) = 0 , \tag{12}$$

where $f_n(\phi_n,\phi_p,\varphi) = \nabla\cdot(\mu_n\nabla n - \mu_n n\nabla\varphi) - (R-G)$. Using the Taylor series, the formula (12) can be expanded as (13), which ignores the second and higher order items:

$$\begin{aligned} & F_n\left(\phi_n,\phi_p,\varphi\right) + \left.\frac{\partial F_n\left(\phi_n,\phi_p,\varphi\right)}{\partial\phi_n}\right|_{\substack{\phi_n=\phi_n{}^{m,l}\\ \phi_p=\phi_p{}^{m,l}\\ \varphi=\varphi^{m,l}}} \left(\phi_n{}^{m,l+1} - \phi_n{}^{\mathrm{m},l}\right) + \\ & \left.\frac{\partial F_n\left(\phi_n,\phi_p,\varphi\right)}{\partial\phi_p}\right|_{\substack{\phi_n=\phi_n{}^{m,l}\\ \phi_p=\phi_p{}^{m,l}\\ \varphi=\varphi^{m,l}}} \left(\phi_p{}^{m,l+1} - \phi_p{}^{m,l}\right) + \\ & \left.\frac{\partial F_n\left(\phi_n,\phi_p,\varphi\right)}{\partial\varphi}\right|_{\substack{\phi_n=\phi_n{}^{m,l}\\ \phi_p=\phi_p{}^{m,l}\\ \varphi=\varphi^{m,l}}} \left(\varphi^{m,l+1} - \varphi^{m,l}\right) = 0. \end{aligned} \tag{13}$$

The superscript m is used to indicate the variables at the time of $m\Delta t$, and l presents the variables obtained by the l_{th} iteration. Applying the Galerkin weighted-residual method, the formula (13) can be transformed to a form of equation system.

Repeat the above operations for the hole current continuity equation and Poisson equation, the final system equation (14) can be obtained:

$$\begin{pmatrix} \mathbf{TN} & \mathbf{NP} & \mathbf{NF} \\ \mathbf{PN} & \mathbf{TP} & \mathbf{PF} \\ \mathbf{FN} & \mathbf{FP} & \mathbf{TF} \end{pmatrix} \begin{pmatrix} \phi_n^{m,l+1} - \phi_n^{m,l} \\ \phi_p^{m,l+1} - \phi_p^{m,l} \\ \varphi^{m,l+1} - \varphi^{m,l} \end{pmatrix} = \begin{pmatrix} \mathbf{BN} \\ \mathbf{BP} \\ \mathbf{BF} \end{pmatrix}. \qquad (14)$$

The elemental matrices are defined as follows:

$$\begin{aligned} TN_{i,j} = & \iiint_V \Delta t \mu_n \exp\left(\varphi^{m,l} - \phi_n^{m,l}\right) \nabla N_i \cdot \nabla \phi_n^{m,l} N_j dV - \iiint_V \exp\left(\varphi^{m,l} - \phi_n^{m,l}\right) N_i N_j dV \\ & - \iiint_V \Delta t \mu_n \exp\left(\varphi^{m,l} - \phi_n^{m,l}\right) \nabla N_i \cdot \nabla N_j dV + \Delta t \int N_i \cdot N_j \frac{\partial (G-R)^{m,l}}{\partial \phi_n} dV \end{aligned},$$

$$NP_{ij} = \Delta t \int N_i \cdot N_j \frac{\partial (G-R)^{m,l}}{\partial \phi_p} dV,$$

$$\begin{aligned} NF_{i,j} = & -\iiint_V \Delta t \mu_n \exp\left(\varphi^{m,l} - \phi_n^{m,l}\right) \nabla N_i \cdot \nabla \phi_n^{m,l} N_j dV + \iiint_V \exp\left(\varphi^{m,l} - \phi_n^{m,l}\right) N_i N_j dV \\ & + \Delta t \int N_i \cdot N_j \frac{\partial (G-R)^{m,l}}{\partial \varphi} dV \end{aligned},$$

$$PN_{ij} = \Delta t \int N_i \cdot N_j \frac{\partial (G-R)^{m,l}}{\partial \phi_n} dV,$$

$$\begin{aligned} TP_{i,j} = & \iiint_V \Delta t \mu_p \exp\left(\phi_p^{m,l} - \varphi^{m,l}\right) \nabla N_i \cdot \nabla \phi_p^{m,l} N_j dV + \iiint_V \exp\left(\phi_p^{m,l} - \varphi^{m,l}\right) N_i N_j dV \\ & + \iiint_V \Delta t \mu_p \exp\left(\phi_p^{m,l} - \varphi^{m,l}\right) \nabla N_i \cdot \nabla N_j dV + \Delta t \int N_i \cdot N_j \frac{\partial (G-R)^{m,l}}{\partial \phi_p} dV \end{aligned},$$

$$\begin{aligned} PF_{i,j} = & -\iiint_V \Delta t \mu_p \exp\left(\phi_p^{m,l} - \varphi^{m,l}\right) \nabla N_i \cdot \nabla \phi_p^{m,l} N_j dV - \iiint_V \exp\left(\phi_p^{m,l} - \varphi^{m,l}\right) N_i N_j dV \\ & + \Delta t \int N_i \cdot N_j \frac{\partial (G-R)^{m,l}}{\partial \phi_p} dV \end{aligned},$$

$$FN_{i,j} = \iiint_V \exp\left(\varphi^{m,l} - \phi_n^{m,l}\right) N_i N_j dV,$$

$$FP_{i,j} = \iiint_V \exp\left(\phi_p^{m,l} - \varphi^{m,l}\right) N_i N_j dV,$$

$$\begin{aligned} TF_{i,j} = & -\iiint_V \varepsilon_2 \left[\exp\left(\varphi^{m,l} - \phi_n^{l}\right) + \exp\left(\phi_p^{m,l} - \varphi^{m,l}\right)\right] N_i N_j dV \\ & - \iiint_V \varepsilon_1 \nabla N_i \cdot \nabla N_j dV \end{aligned},$$

$$\begin{aligned} BN_i = & \iiint_V \Delta t \mu_n \exp\left(\varphi^{m,l} - \phi_n^{m,l}\right) \nabla N_i \cdot \nabla \phi_n^{m,l} dV + \iiint_V \Delta t N_i (G-R) dV \\ & - \iiint_V N_i \left[\exp\left(\varphi^{m,l} - \phi_n^{m,l}\right) - \exp\left(\varphi^{m-1} - \phi_n^{m-1}\right)\right] dV \end{aligned},$$

$$\begin{aligned} BP_i = & -\iiint_V \Delta t \mu_p \exp\left(\phi_p^{m,l} - \varphi^{m,l}\right) \nabla N_i \cdot \nabla \phi_p^{m,l} dV + \iiint_V \Delta t N_i (G-R) dV \\ & - \iiint_V N_i \left(\exp\left({\phi_p}^{m,l} - \varphi^{m,l}\right) - \exp\left({\phi_p}^{m-1} - \varphi^{m-1}\right)\right) dV \end{aligned},$$

$$BF_i = \iiint_V \nabla N_i \cdot \nabla \varphi^{m,l} dV + \iiint_V N_i \left[\exp\left(\varphi^{m,l} - \phi_n^{m,l}\right) - \exp\left(\phi_p^{m,l} - \varphi^{m,l}\right) - \Gamma\right] dV.$$

When the norm of the solutions is less than the setting of tolerance, $({\phi_n}^{l+1}, {\phi_p}^{l+1}, \varphi^{l+1})^T$ can be accounted as the approximate solution of the original nonlinear system.

For the analysis of electro-thermal interaction of semiconductor, the heat conduction equation should be solved after the system equation (14) solved by the Newton iterative method. In particular, the heat conduction equation can be solved easily by the SETD method, which is a linear equation system. For the sake of simplicity, this process is omitted over here. But it needs to be stressed that the procedure of heat conduction equation solving should be repeatedly implemented on each iterative process of the Newton iterative method.

B. Circuits with semiconductor devices

For the transient simulation of the MOSFET common source amplifier circuit, the goal is to obtain a solution satisfying both the external circuit constraint and MOSFET physical model equations. Figure 1 shows the configuration of a MOSFET common source amplifier circuit [18]. Two load resistors, R0 and RL, are connected to the transistor. VDD is the voltage imposed on the drain of the MOSFET through R0. The source of the transistor is grounded. The input voltage Vgs is composed of two signals: the DC bias voltage VGG and the AC signal Vg. The output voltage Vds is equivalent to the drain-to-source voltage of the amplifier.

Firstly, the MOSFET in the amplifier can be treated as a system with the input signals Vgs and Vds, and the output signals can be the drain current Id and the heat distribution among the transistor. This multi-physics simulation under a certain input signal can be implemented utilizing the method proposed in Section A. The input voltage Vgs is a given value at a certain moment. Therefore, the transient relationship between drain current and the drain voltage can be described as the following formula (15):

$$I_d = f_t(V_{ds}). \qquad (15)$$

For this common-source amplifier circuit, the constraint equation of the output circuit is as follows:

$$V_{DD} = (I_d + \frac{V_{ds}}{R_L})R_0 + V_{ds}. \qquad (16)$$

Substituting (15) into (16), the coupled circuit equation with physics-based MOSFET model becomes:

$$F_t(V_{ds}) = (f_t(V_{ds}) + \frac{V_{ds}}{R_L})R_0 + V_{ds} - V_{DD} = 0. \qquad (17)$$

Due to the existence of nonlinear system $f_t(V_{ds})$, Newton-Raphson method is employed to solve equation (17). The derivative of this equation has the following form:

$$F_t{}'(V_{ds}) = \left[f_t{}'(V_{ds}) + \frac{1}{R_L} \right] R_0 + 1. \qquad (18)$$

The derivative approximate expression can be defined as the difference between two adjacent time intervals:

$$f_t{}'(V_{ds}) = \frac{I_d - I_{d0}}{V_{ds} - V_{ds0}}, \qquad (19)$$

where $V_{ds0} = V_{ds} - \beta$ and β is a relative tiny value to ensure the accuracy of the approximation.

Use Taylor series expansion for (17), we can get (20):

$$F_t(V_{ds}^l) + F_t{}'(V_{ds}^l)(V_{ds}^{l+1} - V_{ds}^l) = 0. \qquad (20)$$

Take the formula (18) and (19) into (20), we can get Newton iteration:

$$V_{ds}^{l+1} = V_{ds}^{l} - \frac{(I_d^l R_L + V_{ds}^l)R_0 + (V_{ds}^l - V_{DD})R_L}{(I_d^l - I_{d0}^l)R_0 R_L + (R_0 + R_L)(V_{ds}^l - V_{ds0}^l)}(V_{ds}^l - V_{ds0}^l). \tag{21}$$

Then V_{ds}^{l+1} can be obtain, the convergence condition of Newton iteration is:

$$\left| \frac{V_{ds}^{l+1} - V_{ds}^{l}}{V_{ds}^{l+1}} \right| < \tau , \tag{22}$$

τ is the setting value of tolerance. When the criterion is satisfied, this V_{ds}^{l+1} can be accounted as the approximate solution of the circuit at the current time. Then, substituting V_{ds}^{l+1} into the physics-based MOSFET model once again, the actual electro-thermal behavior can be described finally.

For the transient characteristics simulation of the amplifying circuit, the goal is actually to require a transient solution that satisfies both external circuit constraints and the MOSFET model equation. For the voltage control current device, the input voltage and the output current can be written into a certain functional relationship, and then the circuit equation of the external circuit can be used to obtain the corresponding voltage and current by using the Newton method.

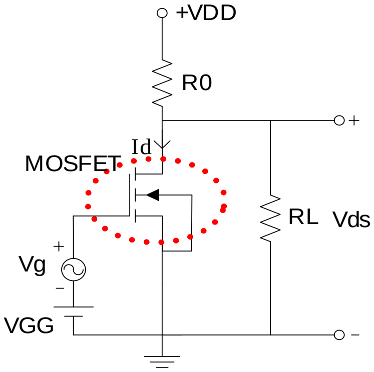

Fig. 1. Common source amplifier circuit with MOSFET.

III. NUMERICAL EXAMPLES

In order to verify the accuracy of the proposed method, the common source amplifier circuit is chosen as the numerical model. The N-channel MOSFET in the circuit is analyzed by solving the drift-diffusion model, and it is convenient to get the thermal characteristics. Here, it should be indicated that all the numerical examples are computed on an Intel(R) Core(TM)2 with 2.83GHz CPU (the results are computed by only one processor) and 8 GB RAM. The tolerance is set to be 10^{-6}.

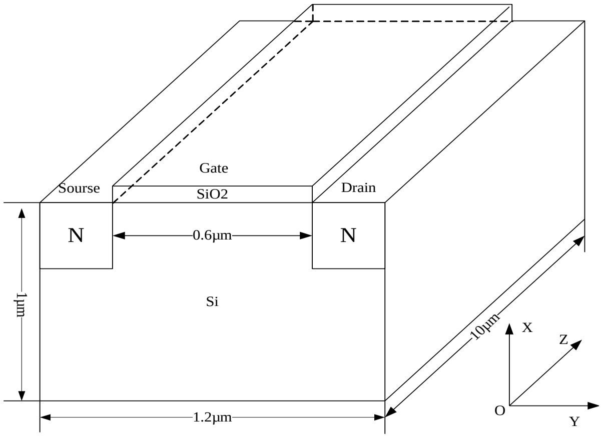

Fig. 2. A 3-D N-channel MOSFET model.

A. Simulation of MOSFET

First, the simulation of a single semiconductor device is implemented to prove the validity of the SETD method. The size of the MOSFET is as shown in Fig. 2, and the doping distribution in Fig. 3. The MOSFET has a size of 1.2*1*10 um, the drain junction depth of 0.3 um, and the oxide thickness of 50nm. The VA characteristic curve is given in Fig. 4, and the comparative results with the COMSOL software have shown the validity of the proposed method. In order to demonstrate the transient characteristic under the electromagnetic pulse with fast rise time, the response with a changing gate voltage has been shown in Fig. 5 and the voltage imposed in the drain is 0.5V. The overshoot current phenomena can be observed in MOSFET transistor from Fig. 5. It takes about additional 15 picoseconds to achieve stability for the particular state change [19]. The calculation of the program takes a little longer than COMSOL, but COMSOL takes up a lot more memory than the program.

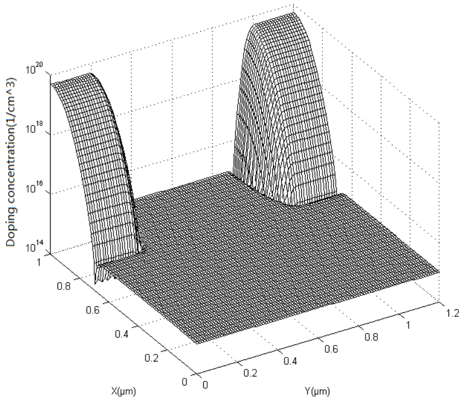

Fig. 3. The doping concentration of MOSFET.

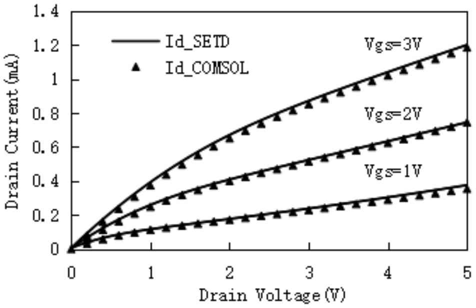

Fig. 4. The VA characteristic curve.

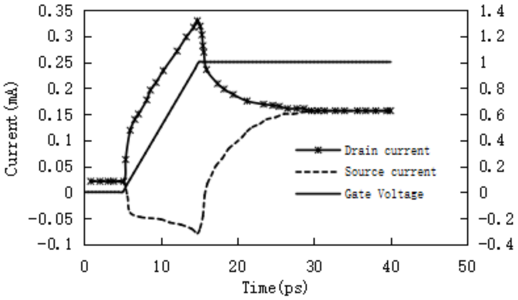

Fig. 5. The transient response with a changing gate voltage.

B. Electron-thermal analysis of circuit

A common source amplifier circuit as shown in Fig. 1 is simulated to analyze its electron-thermal characteristics. In the circuit, the model of MOSFET is the same as the above numerical example, and the simulation of the only semiconductor has been proven to be correct. The electron-thermal analysis of the circuit is following. The remaining setting of the elements in the circuit is as follows: VDD=20 V, R0=20 $K\Omega$, RL=100 $K\Omega$, VGG=1 V. The input signal of Vg and its response with Vds are shown in Fig. 6. The current Id through the MOSFET is shown in Fig. 7 and the transient Maximum temperature varying curve in the MOSFET is shown in Fig. 8. The thermal accumulation effect [6] can be found obviously.

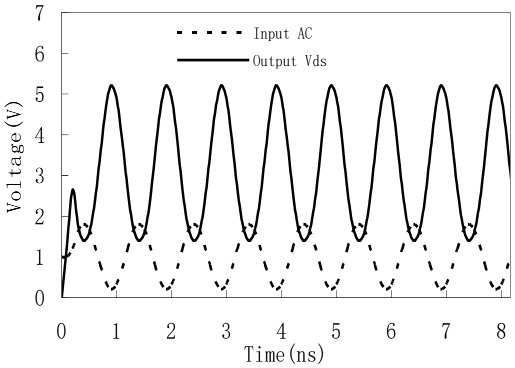

Fig. 6. The input and output voltages with Common Source Amplifier circuit.

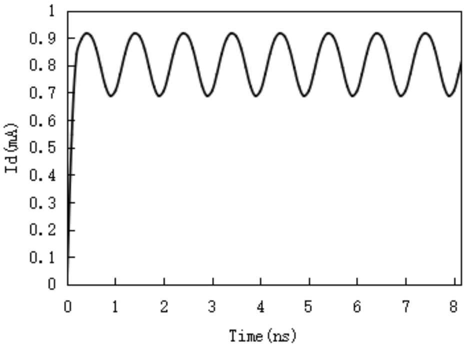

Fig. 7. The current in the MOSFET.

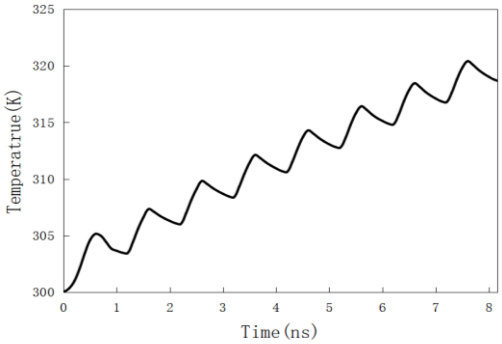

Fig. 8. The transient maximum temperature varying curve.

IV. CONCLUSION

In this paper, the simulation of semiconductor device based on the physical model by the spectral element method in time domain is presented. The VA characteristics of the N-channel MOSFET are analyzed, moreover, the transient response with the changing gate voltage is obtained. Finally, by the co-simulation of an external circuit with physics-based MOSFET model, the behavior of the common source amplifier circuit has been analyzed, the output voltage and current characteristic curves of the common source amplifier circuit has been obtained and the thermal accumulation effect can be found obviously.

ACKNOWLEDGMENT

This work was supported in part by National Key Lab. under Grant 614220503030317, by National Key Lab. of Science and Technology on Space Microwave under Grant 2018SSFNKLSMT-06, Natural Science Foundation of 61871228, the Fundamental Research Funds for the Central Universities No. 30918011202.

REFERENCES

[1] H. A. Mantooth and J. L. Duliere, “A unified diode model for circuit simulation,” *IEEE Trans. Power Electron.*, vol. 12, no. 5, pp. 816-823, Sep. 1997.

[2] K. Kranti, “Microwave-frequency non-linear

universal model for PIN diode," *in Proc. IWPSD*, pp. 119-122, 2007.

[3] C. C. Enz and Y. Cheng, "MOS transistor modeling for RF IC design," *IEEE Trans. Solid-State Circuits*, vol. 35, no. 2, pp. 186-201, Feb. 2000.

[4] M. Pokorny and Z. Raida, "Multi-physics model of Gunn diode," *in Proc.17th Int. Conf. MIKON*, pp. 1-4, May 19-21, 2008.

[5] K. Shinohara and Q. Yu, "Reliability evaluation of power semiconductor devices using coupled analysis simulation," *in Proc. 12th IEEE Intersoc. Conf. Thermal Thermomech. Phenom. Electron. Syst*., pp. 1-9, June 2-5, 2010.

[6] Z. Ren, W. Y. Yin, Y. B. Shi, and Q. H. Liu, "Thermal accumulation effects on the transient temperature responses in LDMOSFETs under the impact of a periodic electromagnetic pulse," *IEEE Trans. Electron Devices*, vol. 57, no. 1, pp. 345-352, Jan. 2010.

[7] S. Yan, A. Greenwood, J. M. Jin, "Modeling of plasma formation during high-power microwave breakdown in air using the discontinuous Galerkin time-domain method," [J]. *IEEE Journal on Multiscale & Multiphysics Computational Techniques*, 1:2-13, 2017.

[8] X. Chen, J. Chen, K. Huang, and X. B. Xu, "A circuit simulation method based on physical approach for the analysis of Mot_bal99lt1 p-i-n diode circuits," *IEEE Trans. Electron Devices*, vol. 58, no. 9, pp. 2862-2870, Sep. 2011.

[9] J. Chen, X. Chen, C. J. Liu, K. Huang, and X. B. Xu, "Analysis of temperature effect on p-i-n diode circuits by a multiphysics and circuit cosimulation algorithm," *IEEE Trans. Electron Devices*, vol. 59, no. 11, pp. 3069-3077, Nov. 2012.

[10] J.-H. Lee and Q. H. Liu, "A 3-D spectral-element time-domain method for electromagnetic simulation," *IEEE Trans. Microw. Theory Tech.*, vol. 55, no. 5, pp. 983-991, May 2007.

[11] I. Mahariq, M. Kuzuoglu, I. H. Tarman, and H. Kurt, "Photonic nanojet analysis by spectral element method," *IEEE. Photonics Journal*, vol. 6, no. 5, pp. 85-90, Oct. 2014.

[12] J.-H. Lee and Q. H. Liu, "An efficient 3-D spectral-element method for Schrödinger equation in nanodevice simulation," *IEEE Trans. Computer Aided Design of Integrated Circuits and Systems*, vol. 24, no. 12, pp. 1848-1858, Dec. 2005.

[13] Y. Sheng, K. Xu, D. Wang, and R. S. Chen, "Performance analysis of FET microwave devices by use of extended spectral-element time-domain method," *International Journal of Electronics*, vol. 100, no. 5, pp. 699-717, May 2013.

[14] K. Xu, R. S. Chen, Y. Sheng, P. Fu, C. Chen, Q. Yan, and Y. Y. Yu, "Transient analysis of microwave Gunn oscillator using extended spectral element time domain method," *Radio Science*, vol. 46, no. 5, pp. 369-380, Sep. 2011.

[15] R. E. Bank, D. J. Rose, and W. Fichtner, "Numerical methods for semiconductor device simulation," *IEEE Trans. Electron Devices*, vol. 30, no. 9, pp. 1031-1041, Sep. 1983.

[16] W. Fichtner, D. J. Rose, and R. E. Bank, "Semiconductor device simulation," *IEEE Trans. Electron Devices*, vol. 30, no. 9, pp. 1018-1030, Sep. 1983.

[17] S. Rzepka, K. Banerjee, E. Meusel, and C. Hu, "Characterization of self-heating in advanced VLSI interconnect lines based on thermal finite element simulation," *IEEE Trans. Compon. Packag. Manuf. Technol. A*, vol. 21, no. 3, pp. 406-411, Sep. 1998.

[18] R. Sayyah, M. Hunt, T. Macleod, and F. D. Ho, "Modeling a common-source amplifier using a ferroelectric transistor," *Integrated Ferroelectrics: An International Journal*, vol. 124, no. 1, pp. 147-156, 2011.

[19] S. Chen, D. Ding, and R. Chen, "A hybrid volume–surface integral spectral-element time-domain method for nonlinear analysis of microwave circuit," [J]. *IEEE Antennas and Wireless Propagation Letters*, vol. 16, pp. 3034-3037, 2017.